Bull. Soc. R. Sci. Liège, 2024, **93**(2), 948–961 *Peer-reviewed conference paper*
doi:10.25518/0037-9565.11933

Exploring Magnetic Coupling of the Solar Atmosphere Through Frequency Modulations of 3-min Slow Magnetoacoustic Waves

Ananya RAWAT[1,2,*] and Girjesh GUPTA[1,*]

[1] Udaipur Solar Observatory, Physical Research Laboratory, Udaipur, India 313001
[2] Department of Physics, Indian Institute of Technology Gandhinagar, India 382355
[*] Corresponding authors: girjesh@prl.res.in; ananyarawat@prl.res.in

Paper presented at the 3rd BINA Workshop on "Scientific Potential of the Indo-Belgian Cooperation", held at the Graphic Era Hill University, Bhimtal (India), 22nd–24th March 2023.

Abstract

Coronal fan loops rooted in a sunspot umbra show outward propagating waves with a subsonic phase speed and a period around 3 min. However, their source region in the lower atmosphere is still ambiguous. We performed multi-wavelength observations of a clean fan loop system rooted in a sunspot utilizing data from the Interface Region Imaging Spectrograph (IRIS) and the Solar Dynamics Observatory (SDO). We explored the less studied property of frequency modulation of these 3-min waves from the photosphere to the corona, and identified periodicities in the ranges of 14–20 min, and 24–35 min. Based on our findings, we interpret that the 3-min slow waves observed in the coronal fan loops are driven by 3-min oscillations observed at the photospheric footpoints of these fan loops in the umbral region. We also investigated possible connections between the 3-min and 5-min oscillations observed at the photosphere, which are still poorly understood. Our results provide clear evidence of magnetic coupling of the solar umbral atmosphere through the propagation of 3-min waves along the fan loops at different atmospheric heights.

Keywords: Sun: corona – Sun: chromosphere – Sun: photosphere – sunspot – waves

1. Introduction

Magnetohydrodynamic (MHD) waves and oscillations are widespread in the solar atmosphere. The propagation properties of these waves were first reported by Ofman and Davila (1997) in polar coronal holes, and by Nakariakov et al. (1999) and De Moortel et al. (2002a) in coronal loops. Detailed information on their characteristics can be found in Khomenko and Collados (2015), Banerjee et al. (2011, 2021), and Jess et al. (2023) for sunspot regions, coronal hole regions, and the lower atmosphere, respectively, to name a few. Recently, numerous studies have been dedicated to identifying observational evidence of wave damping along various structures in the solar atmosphere (e.g. Hahn et al., 2012; Morton et al., 2014; Gupta, 2014; Krishna Prasad et al., 2014; Gupta, 2017; Grant et al., 2018; Gupta et al., 2019). Details about

the current status of the wave heating mechanism of solar corona can be found in recent reviews such as De Moortel and Nakariakov (2012), Van Doorsselaere et al. (2020) etc. Despite the abundance of reports on the propagation and damping characteristics of waves in different layers of the solar atmosphere, observational reports on their generation and source regions remain scarce.

In the lower atmosphere, sunspot regions generally show strong power in the 5-min oscillation bands and significant power in the 3-min oscillation bands at the photosphere (Bellot Rubio et al., 2000). However at heights above the temperature minimum, 3-min oscillations dominate over 5-min oscillations (e.g., Löhner-Böttcher, 2016). In the chromosphere, flashes are observed at random locations in the umbra with a period of about 3 min (Beckers and Tallant, 1969). These flashes are often interpreted as signatures of upward propagating magnetoacoustic shock waves (for further details, see Centeno et al., 2006).

In the corona, fan loops rooted in a sunspot umbra exhibit a continuous presence of propagating disturbances with periods of about 3 min (e.g. De Moortel et al., 2002b). Similar propagating disturbances with a period of about 15 min are also observed along structures in coronal holes (e.g. DeForest and Gurman, 1998; Gupta et al., 2010). These propagating disturbances have subsonic speeds and are often interpreted as propagating slow magnetoacoustic waves (e.g. Kiddie et al., 2012; Gupta et al., 2012). These 3-min slow magnetoacoustic waves also exhibit amplitude modulations with periods in the range of 20–30 min (Sharma et al., 2020) and frequency modulations (Sych et al., 2012). However, observational evidence of their source region is still very rare (e.g. Jess et al., 2012; Krishna Prasad et al., 2015).

In the sunspots, umbral flashes have been observed to influence the propagation properties of various sunspot waves as noted by Sharma et al. (2017). Jess et al. (2012) observed that coronal fan loops rooted in the umbral dots at the photosphere exhibit enhanced power in 3-min oscillations. Krishna Prasad et al. (2015) concluded that 3-min slow magnetoacoustic waves in the coronal fan loops are externally driven by photospheric p-modes. Conversely, Kobanov et al. (2013) and Chae et al. (2017) found no evidence of photospheric and coronal connections. Recently, Rawat and Gupta (2023, hereafter referred to as RG23) carried out a detailed investigation to identify the source region of 3-min waves and oscillations observed in the upper atmosphere. They provided a comprehensive understanding of their source region at the photosphere.

In this study, we present a multi-wavelength analysis of the propagation of 3-min slow magnetoacoustic waves from the photosphere to the corona along fan loop structures rooted within a sunspot umbra. Coronal fan loops are characterized as steady, quiescent, and long loops. Their thermal properties are described in Ghosh et al. (2017). Our primary objective is to probe the source region of these waves in the photosphere, and thereby explore the magnetic connectivity of the solar atmosphere. We achieve this by examining the less explored frequency modulation properties of 3-min waves, which complement results provided by RG23. The observational details are presented in Section 2, followed by the data analysis and results in Section 3. We conclude with the discussion and summary in Section 4.

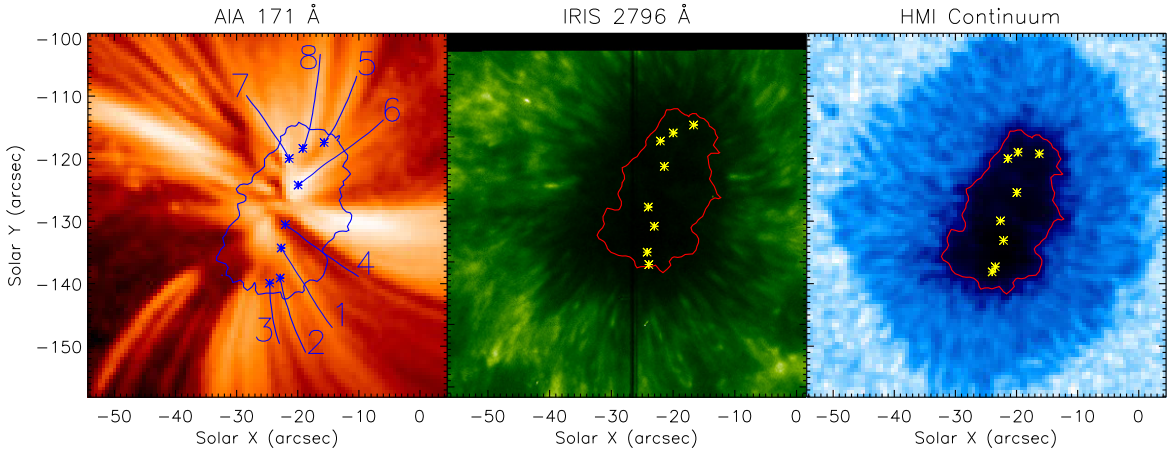

Figure 1: Images of sunspot observed from different AIA, IRIS, and HMI passbands, as labeled. The fan loop system is observed in the AIA 171 Å passband. Identified loop locations are marked with asterisks (✳). Additionally, traced coronal loops are also drawn in the AIA 171 Å passband for visualization purposes only. Contours indicate the umbra-penumbra boundary, as obtained from the HMI continuum image.

2. Observations

We utilized multi-wavelength observations of a sunspot belonging to the NOAA 12553 active region for a duration of four hours on June 16, 2016, starting at 07:19:13 UT. The sunspot was observed by the Atmospheric Imaging Assembly (AIA; Lemen et al., 2012) and the Helioseismic and Magnetic Imager (HMI; Scherrer et al., 2012), both onboard the Solar Dynamics Observatory (SDO; Pesnell et al., 2012), as well as by the Interface Region Imaging Spectrograph (IRIS; De Pontieu et al., 2014). The sunspot region is depicted in Fig. 1 for AIA, IRIS, and HMI passbands as labeled. Additionally, we utilized data obtained from the AIA 193 Å, AIA 304 Å and AIA 1700 Å passbands, as well as from the HMI Dopplergram for our study purpose. Details on data preparation are provided in RG23.

3. Data Analysis and Results

Figure 1 shows the analyzed fan loop structures in the AIA 171 Å passband. Asterisks (✳) indicate the coronal foot-points of fan loops in the AIA 171 Å image. The locations where the loops appear to originate from in the coronal AIA 171 Å image are considered as the foot-points of the loops in the corona. These locations are used as a reference for identifying the locations of these loops in the lower solar atmosphere (further details on the methodology are provided in RG23). Identified loop locations in the lower atmosphere are marked with asterisks. In this study, we identified eight fan loops emanating from the sunspot umbra and labeled them accordingly. Associated coronal loops are also drawn for visualization purposes only. While we analyzed all the identified fan loop locations, we only present here results from loop foot-point 6 as a representative example. Results from all the other loop foot-points are summarized

Table 1: Frequency modulation periods (min) of the 3-min oscillations observed in various fan loop locations at different atmospheric heights, as marked in Fig. 1.

Passbands (Å)	loop 1	loop 2	loop 3	loop 4	loop 5	loop 6	loop 7	loop 8
AIA 193	14, 34	17, 34	15, 30	17, 27	18, 40	19, 26	19, 34	15, 34
AIA 171	15, 27	18, 34	15, 34	15	40	19, 34	20, 34	15, 34
AIA 304	20, 34	18, 30	15, 34	16	18, 40	18, 27	19, 30	34
IRIS 2796	13, 30	20, 30	18, 34	16, 28	40	18, 27	19, 30	16, 34
AIA 1700	16, 30	17, 30	17	14, 30	19, 40	19, 30	20, 30	24, 30
HMI continuum	17, 34	34	18, 35	13, 34	14, 30	17, 30	24, 40	20, 34
HMI Dopplergram	20, 30	27, 40	27	13, 30	14, 30	17, 34	20, 34	20, 40

Table 2: Frequency modulation periods (min) of the 5-min oscillations observed in various fan loop locations at the photosphere, as marked in Fig. 1.

Passbands (Å)	loop 1	loop 2	loop 3	loop 4	loop 5	loop 6	loop 7	loop 8
HMI continuum	30, 41	27	24, 31	22, 35	27, 35	22, 30	19, 27	24, 30
HMI Dopplergram	27, 41	40	19, 23	24, 35	17, 26	20, 30	27, 35	24, 30

in Tables 1 and 2.

Since we have detected significant power in the 3-min period band at each atmospheric height studied here (see details in RG23), we utilize it for detailed investigation. We observe oscillations in the form of unclean wave packets at the coronal foot-point of loop 6 as depicted in the top panel of Fig. 2. This is due to several nearby power peaks present in the period band of 2–3.8 min as explained in RG23.

3.1. Wavelet analysis

In the top panel of Fig. 2, we plot the 16-min background-subtracted light curve of the loop 6 foot-point, obtained from the AIA 171 Å passband.

The 16-min background was obtained by applying an 80-point (16-minute) running average to the light curve under study. In the bottom-left panel of Fig. 2, we present the wavelet power spectrum of the same background-subtracted light curve. To generate the wavelet power spectrum, we utilize a tool developed in IDL® by Torrence and Compo (1998). The left panel displays the wavelet power spectrum with time on the x-axis and period on the y-axis. This graph clearly shows the changes in the oscillatory power over time. The cross-hatched area within this panel is called the cone-of-influence (COI), indicating the region where the transform is affected by edge effects. Oscillation periods in this region are considered unreliable. In the right panel of Fig. 2, we present the global wavelet power spectrum, obtained by averaging over the time domain of the wavelet transform.

We extract the 2–3.8 min period window from the wavelet power spectrum as indicated by the blue colored box in the bottom-left panel of Fig. 2. This enables us to delve into the more

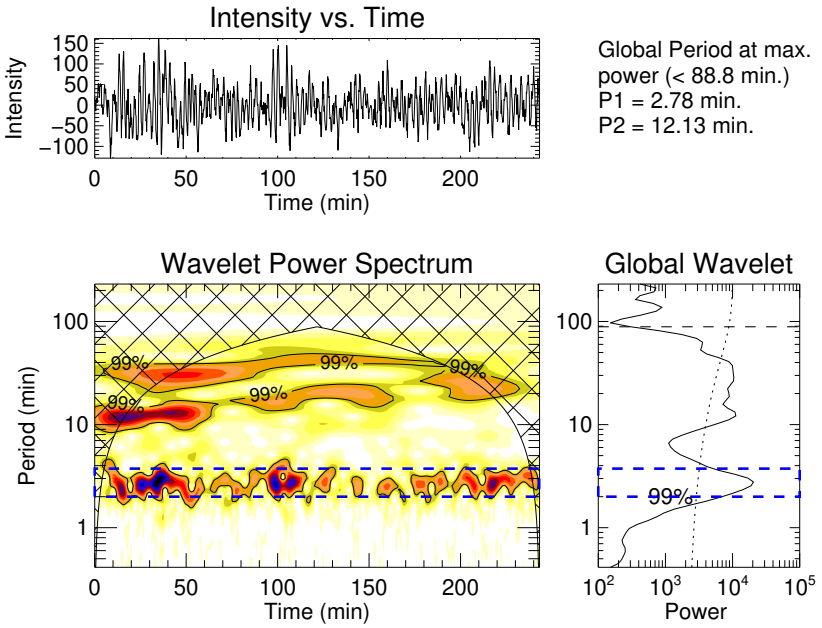

Figure 2: (*top*) The 16-min background-subtracted light curve obtained at the coronal foot-point of loop 6 from the AIA 171 Å passband. (*bottom left*) The color-coded wavelet power spectrum of the background-subtracted light curve with 99% confidence-level contours. The time axis starts at 7:19 UT. Different color contours represent varying power densities, with blue indicating the highest. The cross-hatched area denotes the cone-of-influence. (*bottom right*) The global wavelet power spectrum. The thin black dashed line indicates the maximum detectable period while the dotted line indicates the 99% confidence level. Periods P1 and P2 are the locations of first two maxima in the global wavelet spectrum. The over-plotted blue colored box indicates the period window extracted to obtain detailed information about the 3-min oscillations.

detailed properties of the 3-min oscillations as described in the following subsection.

3.2. Frequency modulations

To determine the frequency modulation of the 3-min waves, we initially derived the wavelet spectrum of the background-subtracted light curves for all the passbands. We then smoothed the wavelet spectrum by applying a seven-point running average along the time axis and a three-point one along the period axis. From this smoothed wavelet spectrum, we extracted the 2–3.8 min period window. Within this subset we further extracted the period at which power is maximum in each time frame. Following the same procedure, we obtained the period or frequency variation of the 3-min oscillation with time at all the atmospheric heights. The variations of the period with time (i.e., frequency modulations) are plotted in the left panels of Fig. 3 for all the passbands, as labeled.

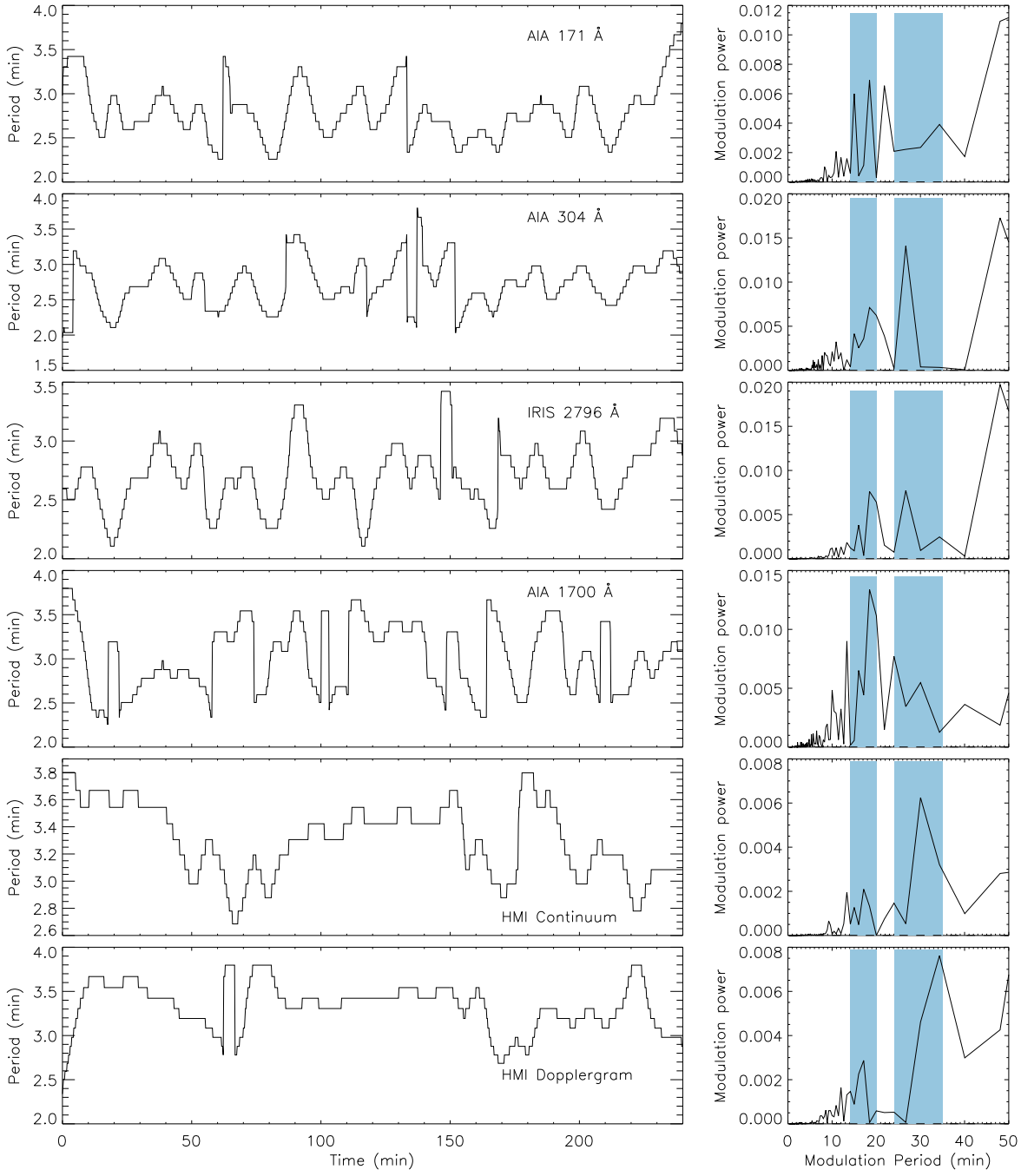

Figure 3: (*left*) The frequency modulations of the 3-min oscillations extracted from the wavelet spectrum for different passbands as labeled. (*right*) The FFT power spectrum of corresponding frequency modulation curves. Shaded regions in sky blue highlight the dominant modulation periods observed at different atmospheric heights.

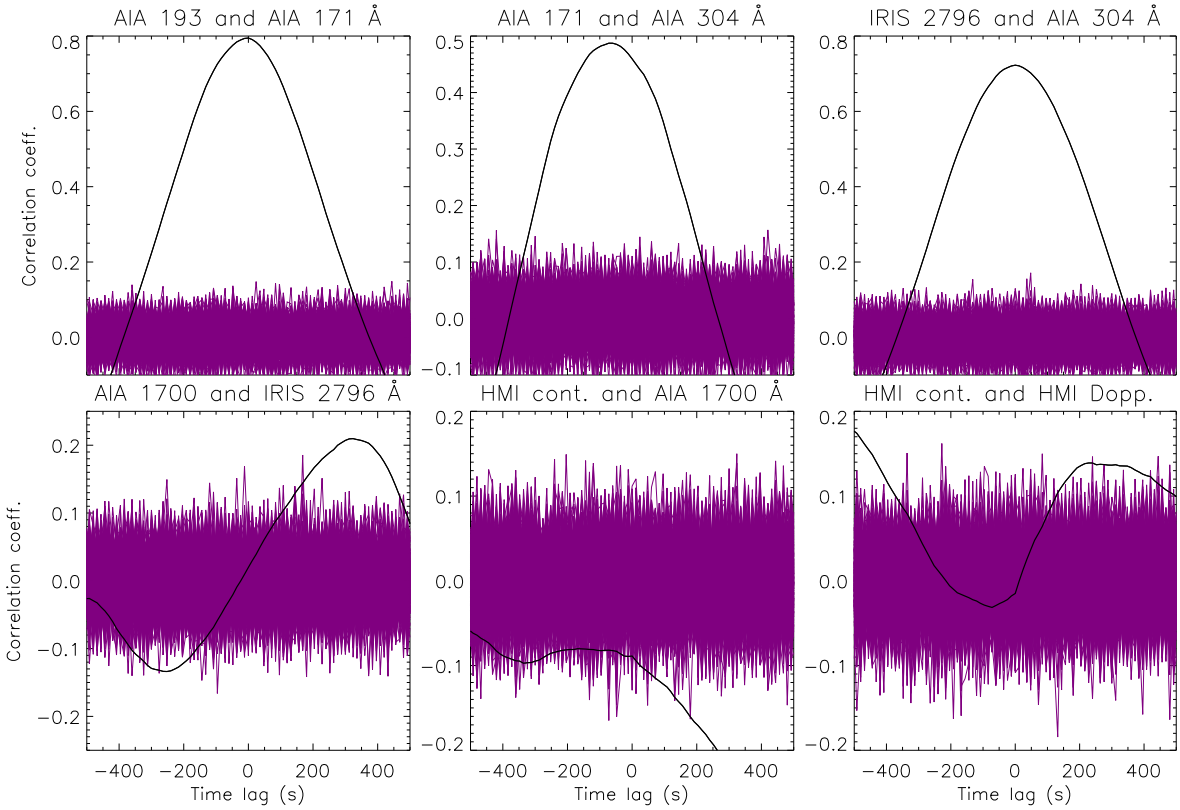

Figure 4: Correlation coefficients for different time lags obtained between frequency modulation curves for different atmospheric heights, as labeled. Purple lines indicate the error range.

We also obtained the FFT power spectrum of frequency modulations and plotted it in the right panels of Fig. 3. In these panels, we can see that the dominant 3-min frequency modulation periods are approximately in the 14–20 min and 24–35 min ranges, which are consistently present in all the layers of the solar atmosphere. These modulation periods are depicted as shaded regions in the right panel of Fig. 3. The similarity in modulation periods indicates that the 3-min oscillations are essentially coupled together across the different atmospheric layers. This provides clear evidence of upward propagating waves from the photosphere to the corona along the observed fan loop locations. We furthermore notice that power peaks within the 24–35 min shaded region are shifting towards the left for coronal heights. However, it is important to notice that these shifts are within the error range and would require high-frequency resolution data to deduce any significant shifts in modulation periods.

We also conducted a cross-correlation analysis on frequency modulation curves obtained at different atmospheric heights with their nearest atmospheric layers. The resulting correlation curves are presented in Fig. 4. The obtained correlations exhibit a similar pattern to those obtained for amplitude modulations in RG23, although the correlation values are smaller. To assess the reliability of the correlation coefficient values, we performed a randomization bootstrap analysis (see details in RG23). We clearly see that correlation values are either above or below the error range provided by the bootstrap analysis (shown in purple). We also noticed that the correlation between the modulation curves decreases as we move into the lower atmosphere.

For pairs of AIA 1700 Å and HMI continuum, and of HMI continuum and Dopplergram, correlations are poor and fall within the error range. However, for the IRIS 2796 and AIA 1700 Å pair, correlation is weak but exceeds the error range. Therefore, this analysis provides evidence of magnetic connectivity of the solar atmosphere from the temperature minimum region (AIA 1700 Å) to the corona (AIA 171 and 193 Å). However, all frequency modulation curves show similar modulation periods. Taken together, these findings provide clear evidence of magnetic connectivity of the whole solar atmosphere.

3.3. Relation between the 3-min and the 5-min oscillations at the photosphere

Since both the 3-min and the 5-min oscillations are observed at the photosphere (e.g., Centeno et al., 2006; Rawat and Gupta, 2023), we also obtained frequency modulations of 5-min oscillation at the photosphere to examine any relation between the two oscillations. To achieve this, we performed a similar wavelet analysis by selecting the period window between 4.1–6.2 min. In Fig. 5, we present the frequency modulations of the 5-min oscillations as labeled (panel a), and their respective FFT power spectrum (panel b). From the plots, we observe power peaks between 19–24 min and 28–32 min periods, which are highlighted as shaded regions from both the HMI continuum and Dopplergram, as labeled. Additionally, we notice a weak modulation period of around 16–17 min in both passbands.

The correlation between modulations from both the HMI passbands for 5-min oscillations is about 0.64 with a time lag of ≈ 24 s, as shown by the green line in Fig. 5(c). When comparing the modulation periods of both 3-min and 5-min oscillations from Figs. 3 and 5(b), we observe that longer modulation periods above 25 min and weaker modulation periods around 16–17 min are present in both oscillations. Therefore, we conducted a correlation analysis to verify any coupling between these modulations, and thus any coupling between 3-min and 5-min oscillations. In Fig. 5(c), we plot the correlation coefficients with respect to time lags obtained between frequency modulations of 3-min and 5-min oscillations observed from the HMI continuum and Dopplergram, as labeled. The maximum correlation coefficient between the modulations of the 3-min and 5-min oscillations from the HMI continuum data is about 0.46 for a time lag of ≈ -24 s whereas the corresponding correlation obtained from the HMI Dopplergram data is very small and within the error range. Here again, the error range is obtained from randomization bootstrap analysis as before. Therefore, these correlation values indicate poor or weak connection between 3-min and 5-min oscillations at the photosphere. Hence, any connection between them at the photosphere remains unclear, as also noticed by RG23, and thus demands a dedicated study to explore their connection in detail.

We also performed a similar analysis on other fan loops identified in Fig. 1. A summary of the frequency modulation periods obtained for 3-min and 5-min oscillations at various atmospheric heights for all eight loops are provided in Tables 1 and 2, respectively. Obtained results suggest more or less similar statistics as presented by RG23 from amplitude modulations. Upon comparison, we find that periods of amplitude and frequency modulations exhibit similar modulation periods, with at least one common modulation period observed at all atmospheric heights. These results indicate that 3-min waves observed in coronal fan loops originate at the

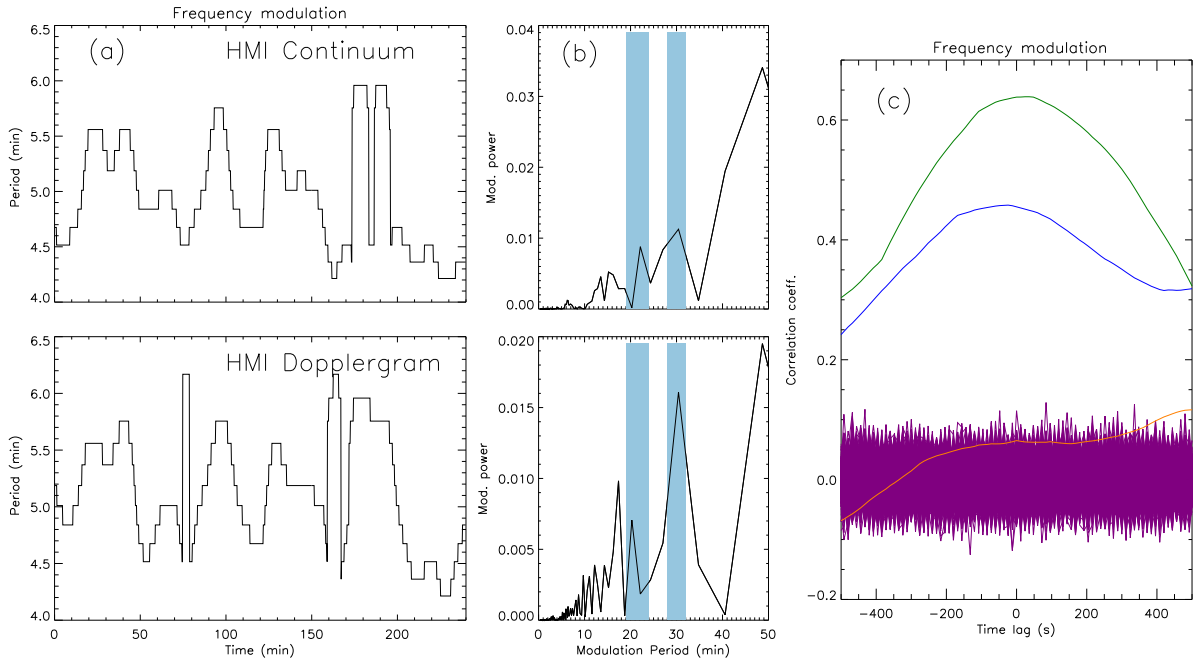

Figure 5: (a) Frequency modulations of the 5-min oscillations at the photosphere as labeled. (b) The FFT power spectrum of corresponding modulations. Shaded regions in sky blue color highlight dominant modulation periods. (c) Correlations with respect to time lags obtained between frequency modulations of the 3-min and the 5-min oscillations. Green, blue, and orange lines show correlations obtained between frequency modulation curves of the 5-min oscillations from the HMI continuum and Dopplergram, 3-min and 5-min oscillations from the HMI continuum, and 3-min and 5-min oscillations from the HMI Dopplergram, respectively. Purple lines indicate the error range.

photosphere and propagate upward, based on the presence of at least one common modulation period at all atmospheric heights (e.g., Krishna Prasad et al., 2015; Rawat and Gupta, 2023). We furthermore find several common modulation periods between amplitude and frequency modulations at all atmospheric heights, implying that these modulations are also interconnected. Moreover, we noted strong anti-correlations between amplitude and frequency modulations at chromospheric heights (AIA 1700 Å or IRIS 2796 Å) for all the loops. The results from all the loops again provide clear evidence of the magnetic connectivity of the entire solar atmosphere.

4. Discussion and Summary

In this work, we utilized less-explored frequency modulations of 3-min oscillations and found modulation periods in the range 14–20 min and 24–35 min throughout the photosphere to the corona along fan loops. These modulations are correlated with each other at different atmospheric heights. Therefore based on our these findings, we conclude that 3-min waves in the upper atmosphere are a direct result of 3-min oscillations observed at the photospheric

umbral region similar to the findings of RG23. It should be noted that in the solar atmosphere, density difference at different heights act as a barrier, causing a fraction of waves to be reflected back. Additionally, due to a decrease in density, steepening of amplitude takes place, resulting in shock formation in the lower atmosphere. This also affects the correlation values of frequency modulations between those heights. These effects are clearly observed in correlations for passband pairs where sharp changes in densities are expected. Both of these results strengthen our claim that 3-min waves observed in the coronal fan loops are driven by 3-min oscillations observed at the photospheric foot-points of these fan loops within the umbra and support the models of Fleck and Schmitz (1991) and Centeno et al. (2006).

Contrary views exist on any connection between 3-min and 5-min oscillations observed in the solar atmosphere (e.g., Krishna Prasad et al., 2015; Chae et al., 2017). In this work, we found a poor correlation between the modulations of 3-min and 5-min oscillations at the photosphere. Therefore, any connection between 3-min and 5-min oscillations at the photosphere remains ambiguous and is a topic of future interest and exploration. Moreover, during the analysis, we also noted that in comparison to amplitude modulation, frequency modulation is a more direct method to probe the connectivity of the solar atmosphere, especially to examine the connection between 3-min and 5-min oscillations at the photosphere, as this relation or drift can be directly observed and analyzed with the wavelet tools. However, we need better frequency and spatial resolution data to explore these connections further.

In summary, we investigated the magnetic coupling of the solar atmosphere by analyzing the frequency modulations of 3-min waves observed from the photosphere to the corona. These 3-min waves exhibited periodic modulations in their frequency with periods of about 14–20 min and 24–35 min at all the altitudes. They also showed correlations at different atmospheric heights except at the photosphere. Results reveal that 3-min waves observed in the coronal fan loops are driven by 3-min oscillations observed at the photospheric foot-points of these fan loops in the umbral region. This finding underscores the magnetic coupling of the entire solar atmosphere.

Acknowledgments

The AIA and HMI data utilized in this study are provided courtesy of NASA/SDO and the AIA and HMI consortia. IRIS is a NASA Small Explorer mission developed and operated by LMSAL, with mission operations executed at NASA Ames Research Center. Major contributions to downlink communications are funded by the Norwegian Space Center (NSC, Norway) through an ESA PRODEX contract. Facilities: SDO (AIA, HMI), IRIS.

Further Information

Authors' ORCID identifiers

0009-0005-9936-9928 (Ananya RAWAT)
0000-0002-0437-6107 (Girjesh GUPTA)

Author contributions

AR conducted the data analysis and generated the figures. GG conceptualized the study, conducted the data corrections and supervised the project. Both the authors contributed in paper writing.

Conflicts of interest

The authors declare no conflict of interest.

References

Banerjee, D., Gupta, G. R. and Teriaca, L. (2011) Propagating MHD waves in coronal holes. SSRv, 158, 267–288. https://doi.org/10.1007/s11214-010-9698-z.

Banerjee, D., Krishna Prasad, S., Pant, V., McLaughlin, J. A., Antolin, P., Magyar, N., Ofman, L., Tian, H., Van Doorsselaere, T., De Moortel, I. and Wang, T. J. (2021) Magnetohydrodynamic waves in open coronal structures. SSRv, 217(7), 76. https://doi.org/10.1007/s11214-021-00849-0.

Beckers, J. M. and Tallant, P. E. (1969) Chromospheric inhomogeneities in sunspot umbrae. SoPh, 7, 351–365. https://doi.org/10.1007/BF00146140.

Bellot Rubio, L. R., Collados, M., Ruiz Cobo, B. and Rodríguez Hidalgo, I. (2000) Oscillations in the photosphere of a sunspot umbra from the inversion of infrared Stokes profiles. ApJ, 534(2), 989–996. https://doi.org/10.1086/308791.

Centeno, R., Collados, M. and Trujillo Bueno, J. (2006) Spectropolarimetric investigation of the propagation of magnetoacoustic waves and shock formation in sunspot atmospheres. ApJ, 640, 1153–1162. https://doi.org/10.1086/500185.

Chae, J., Lee, J., Cho, K., Song, D., Cho, K. and Yurchyshyn, V. (2017) Photospheric origin of three-minute oscillations in a sunspot. ApJ, 836(1), 18. https://doi.org/10.3847/1538-4357/836/1/18.

De Moortel, I., Ireland, J., Hood, A. W. and Walsh, R. W. (2002a) The detection of 3 & 5 min period oscillations in coronal loops. A&A, 387, L13–L16. https://doi.org/10.1051/0004-6361:20020436.

De Moortel, I., Ireland, J., Walsh, R. W. and Hood, A. W. (2002b) Longitudinal intensity oscillations in coronal loops observed with TRACE. I. Overview of measured parameters. SoPh, 209(1), 61–88. https://doi.org/10.1023/A:1020956421063.

De Moortel, I. and Nakariakov, V. M. (2012) Magnetohydrodynamic waves and coronal seismology: an overview of recent results. RSPTA, 370, 3193–3216. https://doi.org/10.1098/rsta.2011.0640.

De Pontieu, B., Title, A. M., Lemen, J. R., Kushner, G. D., Akin, D. J., Allard, B., Berger, T., Boerner, P., Cheung, M., Chou, C., Drake, J. F., Duncan, D. W., Freeland, S., Heyman, G. F., Hoffman, C., Hurlburt, N. E., Lindgren, R. W., Mathur, D., Rehse, R., Sabolish, D., Seguin, R., Schrijver, C. J., Tarbell, T. D., Wülser, J. P., Wolfson, C. J., Yanari, C., Mudge, J., Nguyen-Phuc, N., Timmons, R., van Bezooijen, R., Weingrod, I., Brookner, R., Butcher, G., Dougherty, B., Eder, J., Knagenhjelm, V., Larsen, S., Mansir, D., Phan, L., Boyle, P., Cheimets, P. N., DeLuca, E. E., Golub, L., Gates, R., Hertz, E., McKillop, S., Park, S., Perry, T., Podgorski, W. A., Reeves, K., Saar, S., Testa, P., Tian, H., Weber, M., Dunn, C., Eccles, S., Jaeggli, S. A., Kankelborg, C. C., Mashburn, K., Pust, N., Springer, L., Carvalho, R., Kleint, L., Marmie, J., Mazmanian, E., Pereira, T. M. D., Sawyer, S., Strong, J., Worden, S. P., Carlsson, M., Hansteen, V. H., Leenaarts, J., Wiesmann, M., Aloise, J., Chu, K. C., Bush, R. I., Scherrer, P. H., Brekke, P., Martinez-Sykora, J., Lites, B. W., McIntosh, S. W., Uitenbroek, H., Okamoto, T. J., Gummin, M. A., Auker, G., Jerram, P., Pool, P. and Waltham, N. (2014) The Interface Region Imaging Spectrograph (IRIS). SoPh, 289(7), 2733–2779. https://doi.org/10.1007/s11207-014-0485-y.

DeForest, C. E. and Gurman, J. B. (1998) Observation of quasi-periodic compressive waves in solar polar plumes. ApJ, 501, L217–L220. https://doi.org/10.1086/311460.

Fleck, B. and Schmitz, F. (1991) The 3-min oscillations of the solar chromosphere – a basic physical effect? A&A, 250(1), 235–244. https://ui.adsabs.harvard.edu/abs/1991A&A...250..235F.

Ghosh, A., Tripathi, D., Gupta, G. R., Polito, V., Mason, H. E. and Solanki, S. K. (2017) Fan loops observed by IRIS, EIS, and AIA. ApJ, 835(2), 244. https://doi.org/10.3847/1538-4357/835/2/244.

Grant, S. D. T., Jess, D. B., Zaqarashvili, T. V., Beck, C., Socas-Navarro, H., Aschwanden, M. J., Keys, P. H., Christian, D. J., Houston, S. J. and Hewitt, R. L. (2018) Alfvén wave dissipation in the solar chromosphere. NatPh, 14(5), 480–483. https://doi.org/10.1038/s41567-018-0058-3.

Gupta, G. R. (2014) Observations of dissipation of slow magneto-acoustic waves in a polar coronal hole. A&A, 568, A96. https://doi.org/10.1051/0004-6361/201323200.

Gupta, G. R. (2017) Spectroscopic evidence of Alfvén wave damping in the off-limb solar corona. ApJ, 836, 4. https://doi.org/10.3847/1538-4357/836/1/4.

Gupta, G. R., Banerjee, D., Teriaca, L., Imada, S. and Solanki, S. (2010) Accelerating waves in polar coronal holes as seen by EIS and SUMER. ApJ, 718, 11–22. https://doi.org/10.1088/0004-637X/718/1/11.

Gupta, G. R., Del Zanna, G. and Mason, H. E. (2019) Exploring the damping of Alfvén waves along a long off-limb coronal loop, up to 1.4 $R_{\odot}$. A&A, 627, A62. https://doi.org/10.1051/0004-6361/201935357.

Gupta, G. R., Teriaca, L., Marsch, E., Solanki, S. K. and Banerjee, D. (2012) Spectroscopic observations of propagating disturbances in a polar coronal hole: evidence of slow magneto-acoustic waves. A&A, 546, A93. https://doi.org/10.1051/0004-6361/201219795.

Hahn, M., Landi, E. and Savin, D. W. (2012) Evidence of wave damping at low heights in a polar coronal hole. ApJ, 753, 36. https://doi.org/10.1088/0004-637X/753/1/36.

Jess, D. B., De Moortel, I., Mathioudakis, M., Christian, D. J., Reardon, K. P., Keys, P. H. and Keenan, F. P. (2012) The source of 3 minute magnetoacoustic oscillations in coronal fans. ApJ, 757(2), 160. https://doi.org/10.1088/0004-637X/757/2/160.

Jess, D. B., Jafarzadeh, S., Keys, P. H., Stangalini, M., Verth, G. and Grant, S. D. T. (2023) Waves in the lower solar atmosphere: the dawn of next-generation solar telescopes. LRSP, 20(1), 1. https://doi.org/10.1007/s41116-022-00035-6.

Khomenko, E. and Collados, M. (2015) Oscillations and waves in sunspots. LRSP, 12, 6. https://doi.org/10.1007/lrsp-2015-6.

Kiddie, G., De Moortel, I., Del Zanna, G., McIntosh, S. W. and Whittaker, I. (2012) Propagating disturbances in coronal loops: A detailed analysis of propagation speeds. SoPh, 279, 427–452. https://doi.org/10.1007/s11207-012-0042-5.

Kobanov, N. I., Chelpanov, A. A. and Kolobov, D. Y. (2013) Oscillations above sunspots from the temperature minimum to the corona. A&A, 554, A146. https://doi.org/10.1051/0004-6361/201220548.

Krishna Prasad, S., Banerjee, D. and Van Doorsselaere, T. (2014) Frequency-dependent damping in propagating slow magneto-acoustic waves. ApJ, 789, 118. https://doi.org/10.1088/0004-637X/789/2/118.

Krishna Prasad, S., Jess, D. B. and Khomenko, E. (2015) On the source of propagating slow magnetoacoustic waves in sunspots. ApJ, 812(1), L15. https://doi.org/10.1088/2041-8205/812/1/L15.

Lemen, J. R., Title, A. M., Akin, D. J., Boerner, P. F., Chou, C., Drake, J. F., Duncan, D. W., Edwards, C. G., Friedlaender, F. M., Heyman, G. F., Hurlburt, N. E., Katz, N. L., Kushner, G. D., Levay, M., Lindgren, R. W., Mathur, D. P., McFeaters, E. L., Mitchell, S., Rehse, R. A., Schrijver, C. J., Springer, L. A., Stern, R. A., Tarbell, T. D., Wuelser, J.-P., Wolfson, C. J., Yanari, C., Bookbinder, J. A., Cheimets, P. N., Caldwell, D., Deluca, E. E., Gates, R., Golub, L., Park, S., Podgorski, W. A., Bush, R. I., Scherrer, P. H., Gummin, M. A., Smith, P., Auker, G., Jerram, P., Pool, P., Soufli, R., Windt, D. L., Beardsley, S., Clapp, M., Lang, J. and Waltham, N. (2012) The Atmospheric Imaging Assembly (AIA) on the Solar Dynamics Observatory (SDO). SoPh, 275(1-2), 17–40. https://doi.org/10.1007/s11207-011-9776-8.

Löhner-Böttcher, J. (2016) Wave phenomena in sunspots. Ph.D. thesis, Albert Ludwigs University of Freiburg, Germany.

Morton, R. J., Verth, G., Hillier, A. and Erdélyi, R. (2014) The generation and damping of propagating MHD kink waves in the solar atmosphere. ApJ, 784(1), 29. https://doi.org/10.1088/0004-637X/784/1/29.

Nakariakov, V. M., Ofman, L., Deluca, E. E., Roberts, B. and Davila, J. M. (1999) TRACE observation of damped coronal loop oscillations: Implications for coronal heating. Sci, 285, 862–864. https://doi.org/10.1126/science.285.5429.862.

Ofman, L. and Davila, J. M. (1997) Solar wind acceleration by solitary waves in coronal holes. ApJ, 476(1), 357–365. https://doi.org/10.1086/303603.

Pesnell, W. D., Thompson, B. J. and Chamberlin, P. C. (2012) The Solar Dynamics Observatory (SDO). SoPh, 275(1-2), 3–15. https://doi.org/10.1007/s11207-011-9841-3.

Rawat, A. and Gupta, G. R. (2023) Exploring source region of 3-min slow magnetoacoustic waves observed in coronal fan loops rooted in sunspot umbra. MNRAS, 525(4), 4815–4831. https://doi.org/10.1093/mnras/stad2426.

Scherrer, P. H., Schou, J., Bush, R. I., Kosovichev, A. G., Bogart, R. S., Hoeksema, J. T., Liu, Y., Duvall, T. L., Zhao, J., Title, A. M., Schrijver, C. J., Tarbell, T. D. and Tomczyk, S. (2012) The Helioseismic and Magnetic Imager (HMI) investigation for the Solar Dynamics Observatory (SDO). SoPh, 275(1-2), 207–227. https://doi.org/10.1007/s11207-011-9834-2.

Sharma, A., Gupta, G. R., Tripathi, D., Kashyap, V. and Pathak, A. (2017) Direct observations of different sunspot waves influenced by umbral flashes. ApJ, 850(2), 206. https://doi.org/10.3847/1538-4357/aa95c0.

Sharma, A., Tripathi, D., Erdélyi, R., Gupta, G. R. and Ahmed, G. A. (2020) Wave amplitude modulation in fan loops as observed by AIA/SDO. A&A, 638, A6. https://doi.org/10.1051/0004-6361/201936667.

Sych, R., Zaqarashvili, T. V., Nakariakov, V. M., Anfinogentov, S. A., Shibasaki, K. and Yan, Y. (2012) Frequency drifts of 3-min oscillations in microwave and EUV emission above sunspots. A&A, 539, A23. https://doi.org/10.1051/0004-6361/201118271.

Torrence, C. and Compo, G. P. (1998) A practical guide to wavelet analysis. BAMS, 79(1), 61–78. https://doi.org/10.1175/1520-0477(1998)079<0061:APGTWA>2.0.CO;2.

Van Doorsselaere, T., Srivastava, A. K., Antolin, P., Magyar, N., Vasheghani Farahani, S., Tian, H., Kolotkov, D., Ofman, L., Guo, M., Arregui, I., De Moortel, I. and Pascoe, D. (2020) Coronal heating by MHD waves. SSRv, 216(8), 140. https://doi.org/10.1007/s11214-020-00770-y.